Universität Potsdam

Giovanna Guasti, Ralf Engbert, Ralf T. Krampe,
Jürgen Kurths

Phase transitions, complexity, and stationarity in the production of polyrhythms

NLD Preprints ; 57

Phase transitions, complexity, and stationarity in the production of polyrhythms

Giovanna Guasti(1), Ralf Engbert(1)§, Ralf T. Krampe(2)‖, and Jürgen Kurths(1)

(1) *Department of Physics,*
(2) *Department of Psychology,*
University of Potsdam, POB 601553,
D–14415 Potsdam, Germany

NLD Preprint Series (ISSN 1432-2935)
No. 57
Scientific Technical Report

---

§present address: Institute of Psychology, University of Potsdam;
send correspondence to: ralf@ik.uni-potsdam.de
‖present address: Max Planck Institute for Human Development, Lentzeallee 94, D–14195 Berlin, Germany

Contents

1 Introduction

An important aspect of voluntary actions is the timing of elementary movement sequences composing it. The problem of timing was investigated by Stevens already in [1886] through an experiment of synchronization with a metronome and continuation of tapping (i.e. performance of the rhythm without acoustic reference). The control of periodic single–handed movements synchronously to a metronome is theoretically described by linear stochastic processes [Vorberg & Wing 1996].

The timing of movements involving bimanual coordination is investigated using simple rhythm tasks [Deutsch 1983, Jagacinski et al. 1988, Summers et al. 1993, Krampe et al. 1999]. The synchronization with a metronome is described with the help of a first order autoregressive process [Box & Jenkins 1976].

The production of polyrhythm is an ideal task for the investigation of bimanual coordination. In producing a polyrhythm, the hands carry out two different isochronous rhythms, which are in a non–integer relation (for example 3:2, 4:3, 7:5). The difficulty of this task lies in the non–isochrony of the resulting polyrhythm. This leads to strong interaction between the two hands [Krampe et al. 1999] and makes this task suited for the investigation of bimanual coordination. The transition from complicated to easier polyrhythms induced by increasing tempo [Peper et al. 1995] can be modeled using coupled nonlinear oscillators [Haken et al. 1996].

Here, polyrhythmic time series produced by four subjects are analyzed. The tempo of the performance is the control parameter which is externally varied. This analysis extends previous investigations of Krampe et al. [1999] and Engbert et al. [1997], who detected phase transitions in a shorter polyrhythm task (12 cycles) produced on an electric keyboard. In the following, recordings of trials composed of 61 cycles are analyzed in order to check the occurrence of transitions in longer trials. Furthermore, the stationarity of the data will be tested. This will lead to the identification of the control parameter of the dynamical model which describes the qualitative transitions, proposed by Engbert et al. [1997].

In Sec. 2 the experiment will be explained, while the data will be described in Sec. 3. In Sec. 4 the method of symbolic dynamics is introduced and applied to the data. Order–disorder transitions induced by the externally varied tempo are clearly revealed in the symbol patterns. The transitions detected will be quantitatively characterized using the Shannon entropy, in Sec. 5. In Sec. 6, the stationarity of the cycle durations will be tested. Due to the observation of phase transitions in fluctuating data, interesting considerations about the control parameter of the model can be derived (Sec. 7). A representation of the data using relative phases will be proposed in Sec. 8. Finally, in Sec. 9, the results obtained will be discussed.

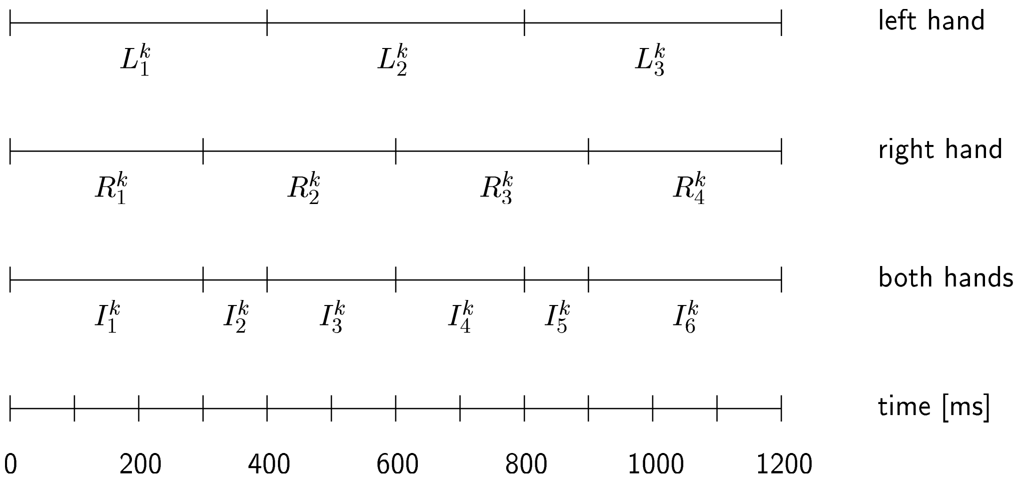

Figure 1: Scheme of a 4:3 polyrhythm with cycle duration of 1200 ms. Right hand and left hand perform 4 and 3 isochronous intervals R and L, respectively. The indices on the bottom indicate the position within the cycle. The latter is indicated by the index k. Each cycle starts and terminates with the simultaneous strokes of both hands. The polyrhythmic time series produced by the two rhythms consist of 6 intervals I_z^k of different durations. Experimentally a small asynchrony I_7^k between the two simultaneous strokes at the end (or at the beginning) of each cycle is additionally recorded.

2 Experiment

A polyrhythmic task consists of two different isochronous rhythms, simultaneously performed by the hands. The two rhythms are in a non–integer relation. In Fig. 1 the scheme of a 4:3 polyrhythm with cycle duration $T = 1200$ ms is shown. In each cycle k ($k = 1, ..., 61$), the right hand produces 4 intervals R_i^k, $i = 1, 2, 3, 4$, while the left hand produces 3 intervals L_j^k, $j = 1, 2, 3$. The cycle starts with two simultaneous strokes. The difficulty of the task is due to the combination of the two rhythms. In fact, in the resulting rhythm the successive strokes are not equidistant, so that the produced polyrhythm is not isochronous.

Polyrhythmic time series produced by four subjects are investigated. The experiment was carried out on electric drums connected with a *Macintosh PowerPC* computer by means of a MIDI–interface. Using this equipment, the data could be recorded with a precision of 1 ms. The experiment is based on the continuation paradigm. At the beginning of each trial, the subject listens to the polyrhythm generated by the computer as long as wished. After that, he or she starts drumming while the computer keeps on producing the polyrhythm for one more cycle before it stops. The data were recorded in three sessions. Each subject performed the

3:4 polyrhythm starting with initially given cycle duration T which ranged from 1100 ms to 2100 ms, varied in steps of 100 ms. For each tempo, about 6 trials, that lasted for 61 cycles, were carried out. At the end of each trial, detailed information about the performance was displayed on the computer screen: the durations of the produced R and L intervals, the averaged cycle duration and the related standard deviation. This way, the subject could receive a feedback about the quality of his or her performance.

3 Data

A time series consists of data recorded during a single trial (61 cycles). Each cycle is composed of 4 intervals produced by the right hand and 3 intervals produced by the left hand, so that the length of the related time series is 244 and 183 intervals, respectively. The data recorded during a trial can be represented separately through two interval sequences corresponding to the intervals produced by the hands.

$$\text{right hand (244 values):} \quad R_1^1,\ R_2^1,\ R_3^1,\ R_4^1,\ R_1^2,\ \ldots\ R_3^{61},\ R_4^{61}\ , \tag{1}$$

$$\text{left hand (183 values):} \quad L_1^1,\ L_2^1,\ L_3^1,\ L_1^2,\ \ldots\ L_2^{61},\ L_3^{61}\ . \tag{2}$$

An example of the raw data is shown in Fig. 2.

4 Symbolic dynamics

Generally, temporal dynamics of deterministic system can be analyzed using a phase space representation. Based on the concept of embedding, the phase space can be reconstructed from experimental data [Takens 1981, Packard et al. 1980, Sauer et al. 1991]. Yet, for physiological systems, due to nonstationarity and noise (intrinsic features of the data produced by many living systems), the related methods are often not suitable [Schreiber & Kantz 1995].

The methods of symbolic dynamics have applications in many fields. In the last years they have proved to be useful also for the analysis of complex systems in various disciplines as geophysics [Witt et al. 1994], astrophysics [Hempelmann & Kurths 1990, Schwarz et al. 1993] and medicine [Kurths et al. 1995, Schiek et al. 1997].

4.1 Symbolic dynamics as a tool for data analysis

Many physical phenomena, continuous in time and space, can be understood by using a formulation in the real or complex field. Yet, a common approach consist in

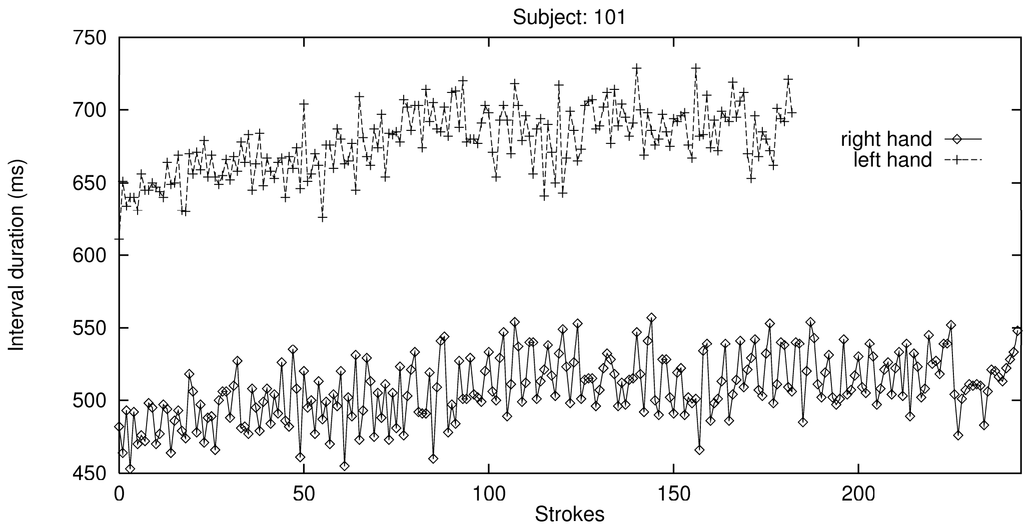

Figure 2: Two examples of R and L intervals. The initially given tempo is $T = 1900$ ms, and the cycle duration averaged over the whole trial is $\langle T \rangle = 2033$ ms. Both time series show fluctuations and periodic structure. The latter is due to the rhythm recurring within each cycle.

discretizing the data in time, using techniques as for example the Poincaré map or the stroboscopic representation.

Many systems continuous in space can be treated in the same way as discrete systems. Once one has chosen a suitable Poincaré surface, a coarse–graining of the phase space can be obtained using a suitable division into cells. Each cell is labeled by a symbol, so that a sequence of symbols is associated to a trajectory in the phase space. This way, a large amount of information is discarded, but some of the robust underlying dynamical properties of the system may be kept [Hao 1989, Hao 1991, Badii & Politi 1997].

In the following, the set X where the motion takes place will be identified with the phase space. Then, a partition $\mathcal{B} = (B_0, ..., B_{b-1})$ of the phase space is introduced, which is formed by b subsets. The set of the labels of the partition's subsets, $A = \{0, 1, ..., b-1\}$, is called an *alphabet*. The partition is defined by the conditions:

$$B_j \cap B_k = \oslash \qquad \text{(disjunction)} \tag{3}$$

for each $j, k = 0, 1, 2, ..., b-1$ with $j \neq k$ and

$$\bigcup_{i=0}^{b-1} B_i = X \qquad \text{(completeness)} \tag{4}$$

Let us consider a system which evolves according to a map

$$\mathbf{x}_i = \mathbf{F}(\mathbf{x}_{i-1}) \tag{5}$$

along an orbit $\mathcal{O}=\{\mathbf{x}_0, \mathbf{x}_1, ..., \mathbf{x}_N\}$ in the phase space X. $s_i \in A$ denotes the index (or symbol) of the subset, visited at the time i. The sequence $\{s_0, s_1, ..., s_N\}$ can be assigned to the trajectory of the system, such that $\mathbf{x}_i \in B_{s_i}, i = 0, ..., N$. To extract the relevant features of the dynamics, a careful choice of the partition $\mathcal{B}$ is necessary. If an infinite sequence of $\{s_1, s_2, s_3...\}$ is such that the initial point $\mathbf{x}_0$ can be uniquely determined by the sequence and vice versa, the partition $\mathcal{B}$ is called a "generating partition". Such a partition exists only in special cases [Beck & Schlögl 1993].

Due to the dynamics, some symbol sequences occur more frequently than others. One can assign to each sequence $S = \{s_0, ..., s_N\}$ a probability $p(s_0, ..., s_N)$ that it is observed. The probability distribution obtained in this way defines a stochastic process [van Kampen 1981], whose features depend on the chosen partition as well as on the underlying dynamics. The probability $p(s_0, ..., s_N)$ can be represented by means of the conditioned probability $p(s_N|s_0, ..., s_{N-1})$, denoting the probability of the event s_N, provided that the sequence $(s_0, ..., s_{N-1})$ has occurred:

$$p(s_0, ..., s_N) = p(s_N|s_0, ..., s_{N-1})p(s_0, ..., s_{N-1}). \tag{6}$$

The stochastic process related to the probability $p(s_0, ..., s_N)$ is called a Markov chain if

$$p(s_N|s_0, ..., s_{N-1}) = p(s_N|s_{N-1}). \tag{7}$$

A *topological Markov chain* is defined by the following property: the transition probability $p(s_N|s_0, ..., s_{N-1})$ is zero, if and only if either it is impossible to reach the cell i_N from the cell i_{N-1}, or the sequence $i_0, i_1, ..., i_{N-1}$ is forbidden.

$$\begin{array}{c} p(s_N|s_0, ..., s_{N-1}) = 0 \\ \text{if and only if} \quad p(s_N|s_{N-1}) = 0 \quad \text{or} \quad p(s_{N-1}|s_0, ..., s_{N-2}) = 0. \end{array} \tag{8}$$

The partition that makes the corresponding stochastic process a topological Markov chain is called a *Markov partition*.

Generally, it cannot be shown whether a Markov partition exists. Even if it exists, there is no constructive method to find it. One can choose between two different strategies: choose a complicated partition in order to get symbol sequences which correspond to simple stochastic processes, or apply straightforward transformations giving symbol sequences with complicated statistical properties [Beck & Schlögl 1993]. In the following, robust characteristics of the dynamics will be extracted from the data by using simple symbolic transformations.

Symbolic dynamics has turned out to be suitable also for the analysis of short polyrhythmic data (12 cycles) [Engbert et al. 1997]. Polyrhythms are sequences of intervals, i.e. discrete time series. They will be shrewdly transformed into symbols in order to extract the dynamical properties of the underlying processes controlling the rhythmic structure within the cycles.

4.2 2–symbols coding

In order to transform the data into symbol sequences, a straightforward coding rule could be used: to each interval, a '0' or a '1' is assigned if its duration is smaller or larger than prescribed ($\frac{T}{4}$ for the right hand and $\frac{T}{3}$ for left hand). T is the initially given cycle duration. Due to the drift of the cycle duration along the trials, through this symbolic transformation, the information regarding the dynamics within the single cycles would be lost. In fact, if the instantaneous realized tempo increases (or decreases) with respect to the initially given tempo, the most of the R and L intervals would be shorter (or longer) than their prescribed value. In this way, the symbol sequences would be mainly composed of a unique symbol, so that the rhythmic structure within a cycle could not be kept by the symbol pattern. The same would happen if the mean realized cycle duration $\langle T \rangle$ would be chosen as reference interval. For these reasons, the intervals R and L are compared with the instantaneous realized cycle duration and transformed into relative deviations [Engbert 1998]. The instantaneous durations t_R^k and t_L^k [1] of the k-th cycle, corresponding to the right and left hand respectively, are computed by summing the subintervals R_i^k and L_j^k within the k–th cycle:

$$\text{right hand:} \qquad t_R^k = \sum_{i=1}^{4} R_i^k \tag{9}$$

$$\text{left hand:} \qquad t_L^k = \sum_{j=1}^{3} L_j^k \; . \tag{10}$$

Then, the relative deviations r_i^k and l_j^k are computed as follows:

$$\text{right hand:} \qquad r_i^k = \frac{4R_i^k - t_R^k}{t_R^k} \; , \qquad i = 1, 2, 3, 4 \; ; \tag{11}$$

[1]Due to the small asynchrony I_7 (see caption of Fig. 2) $t_R^k \neq t_L^k$.

$$\text{left hand:} \qquad l_j^k = \frac{3L_j^k - t_L^k}{t_L^k}\ , \qquad j = 1, 2, 3\ . \tag{12}$$

Such a transformation cannot reveal the overall accuracy of the performance; it rather focuses on the dynamics of the rhythmic structure within the cycles. By means of the transformation defined in Eqs. (11–12), it is possible to quantify the deviation of the produced intervals from the prescribed rhythmic pattern. In this sense, the relative deviations assess locally the accuracy of the performance.

Now, a 2–symbol transformation can be applied to the sequences of the relative deviations according to the following rule:

$$s_n = \begin{cases} 0, & \text{if} \quad r_i^k \text{ or } l_j^k < 0 \\ 1, & \quad \text{otherwise} \end{cases}\ , \tag{13}$$

where $n = 4(k-1) + i = 1,\ 2, 3,\ ...,\ 244$ (right hand) and $n = 3(k-1) + j = 1,\ 2,\ 3,\ ...,\ 183$ (left hand).

Since the threshold in the conditional part of Eq. (13) is constant, this transformation would be static. Nevertheless, in the transformation of Eqs. (11–12), the value of the instantaneous cycle duration, (i.e. the information related to the neighbor intervals) is used. Therefore, the illustrated symbolic transformation is not really static.

The transformed relative deviations can be visualized as follows: white is assigned to the symbol '1' ("too long" interval) and black to the symbol '0' ("too short" interval). This way, for each time series one obtains a sequence of 244 symbols for the right hand and a sequence of 183 symbols for the left hand.

In experimental psychology, it turns out to be difficult to keep the conditions constant during the experiment. In the 3:4 polyrhythm experiment, the initial tempo produced by the computer at the beginning of each trial is the parameter which is externally manipulated. During the synchronization phase, subjects listen to the rhythm produced by the computer as long as they want. During the continuation task (performance of the polyrhythm without any reference), they inevitably deviate from the initially given tempo, so that the realized tempo neither equals the initial one nor it is constant. Engbert [1997], showed that the regularity of patterns where the trials are ordered according the mean realized tempo is higher than if they were sorted with respect to the initially given tempo. The symbol patterns obtained in these two ways are, however, consistent. For these reasons, in the graphic representations of the symbol sequences, they have not been sorted on the x axes according to the initial given tempo T but with respect to the realized tempo averaged over the whole trial $< T >$. In the following, the mean realized tempi will be indicated on the top of the patterns using a ms scale.

The patterns obtained applying the symbol transformation of Eq. 13 on the data produced by the four subjects are shown in (a) in Figs. 3–6 (the plots shown in (b) illustrate results which will be introduced in Sec. 5). Irregularity and order in the pattern correspond to different strategies used in performing the task. If the subject is able to perform the task accurately, the R and L intervals oscillate by chance around the prescribed value. In this case, one observes irregular alternation of white and black symbols in the pattern. Vice versa, a regular or periodic symbol pattern (i.e. a pattern presenting recurrent sub-strings) corresponds to a systematic error. Therefore, regularity in the symbol pattern has to be interpreted as a poor performance and irregularity as a good one.

In Fig. 3 (a) the symbol patterns of the R and L intervals produced by subject 101 are shown. Order–disorder transitions occur in both patterns for increasing values of the control parameter. A first transition occurs around $\langle T \rangle \sim 1300$ ms for both hands. The transition in the pattern of the right hand is sharper than the transition in the pattern of the left hand. For very slow tempi ($\langle T \rangle \geq 2000$ ms) a periodic structure arises again.

One could form the hypothesis that poor performances, that is the occurrence of systematic errors in drumming, is simply due to biomechanical constraints. For example, in very fast trials, the fastest tempo a subject is motorically able to drum correctly could be exceeded. If this happens, one should observe periodicity in the symbol patterns only for faster tempi (short realized cycle duration). On the contrary, periodic structures occur also in an intermediate range of tempi. An example of this behavior is given by subject 102 whose 2–symbol patterns are represented in Fig. 4 (a). The pattern related to the left hand shows a disorder–order transition for $\langle T \rangle \sim 1400$ ms. For slower tempi, the regularity of the pattern reveals a systematic error in the rhythm. This fact excludes the possibility that regular patterns (poor performances) are solely due to motoric restrictions. The pattern of the right hand does not show any clear transition.

The symbol patterns of subject 103, shown in Fig. 5 (a), is similar to the patterns of subject 101. The rhythmic structure of both hands undergoes a transition from a regular (fast tempi) to an irregular (slower tempi) pattern.

In Fig. 6 the data produced by subject 104 are shown. No transitions are visible in dependence on the realized tempo. A periodic structure can be recognized overall in both patterns. In Sec. 8, the graphic representation of the relative phases will focus on dynamical characteristics of bimanual coordination of this subject which cannot be revealed by the symbolic representation of the R and L intervals

The finding of qualitative transitions in the symbol patterns extends one of the main results of the previous study [Engbert et al. 1997], where the same polyrhythmic task was performed on a piano over 12 cycles. The stability of the rhythmic structure along the trial (e.g. the vertical profile of the transitions) demonstrates that the observed transitions exclusively depend on the realized tempo.

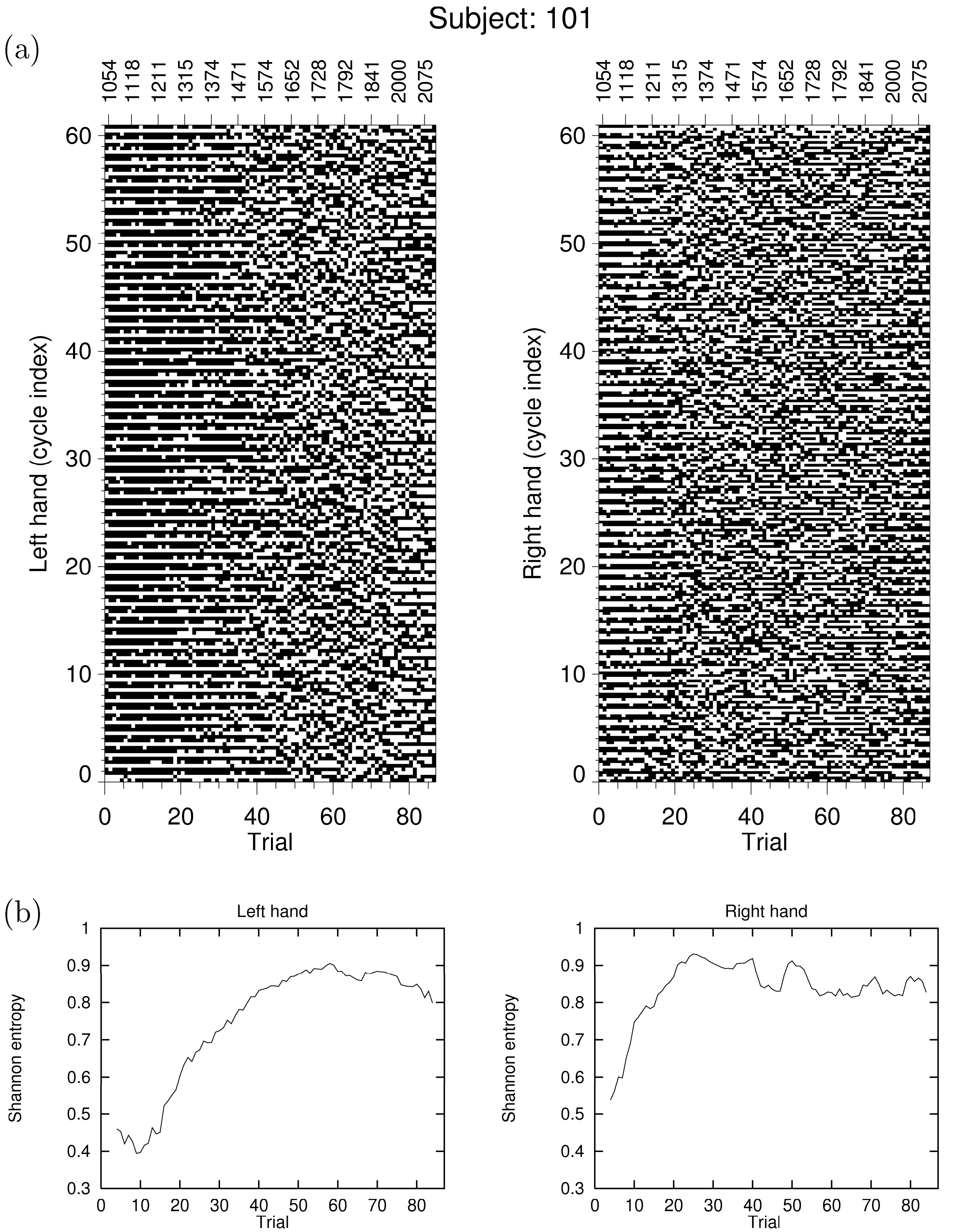

Figure 3: (a) Graphic representation of the symbol patterns obtained using the 2–symbol transformation of Eq. (13) of the R and L intervals. The trials are arranged on the abscissa with respect to the mean realized tempo. The latter is indicated on the top in a ms scale. Time is increasing on the y axes. (b) Shannon entropy of the word distribution characterizing the symbolic sequences represented in (a). For the right and left hand the statistics of the words of length 4 and 3 has been respectively computed.

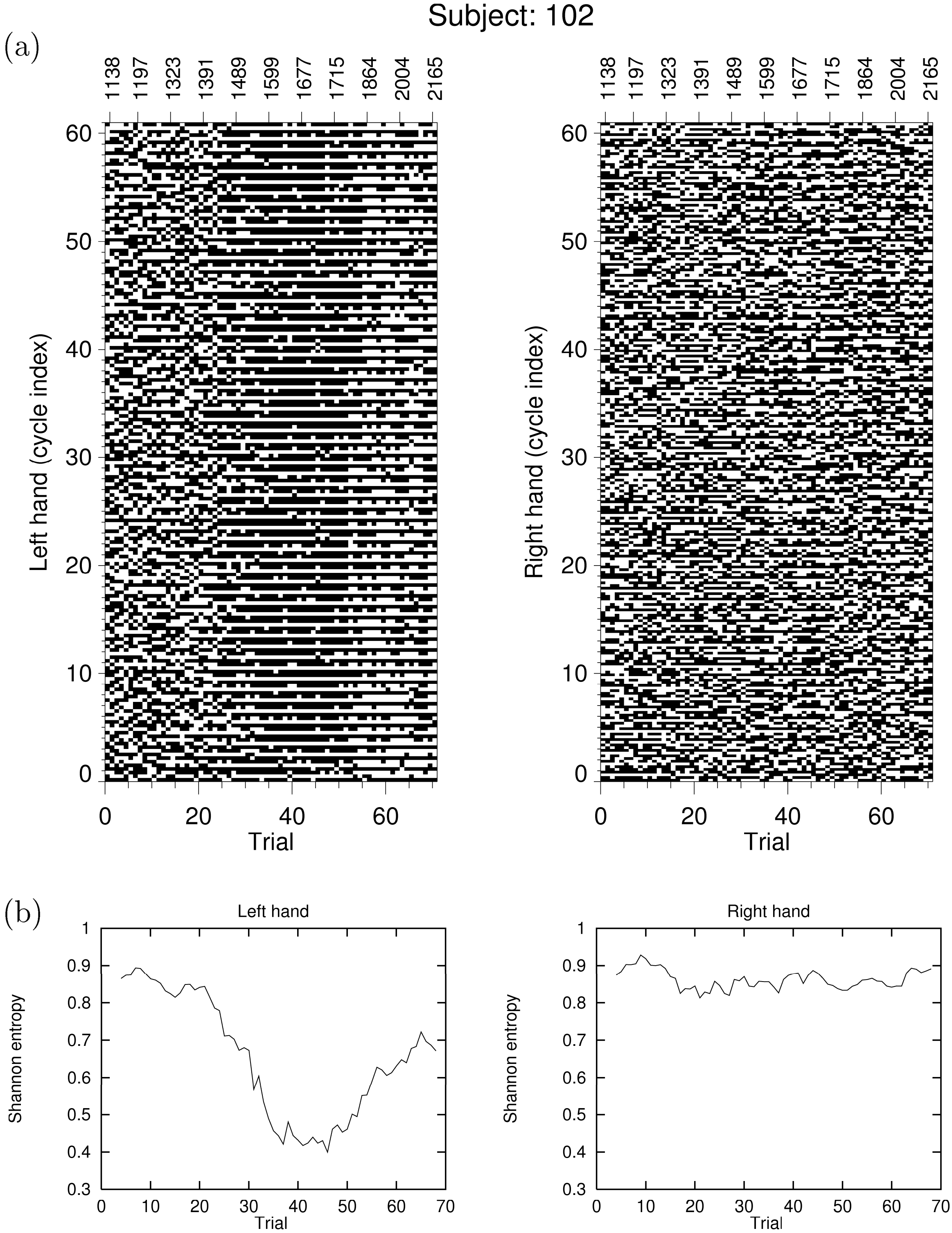

Figure 4: See caption of Fig. 3

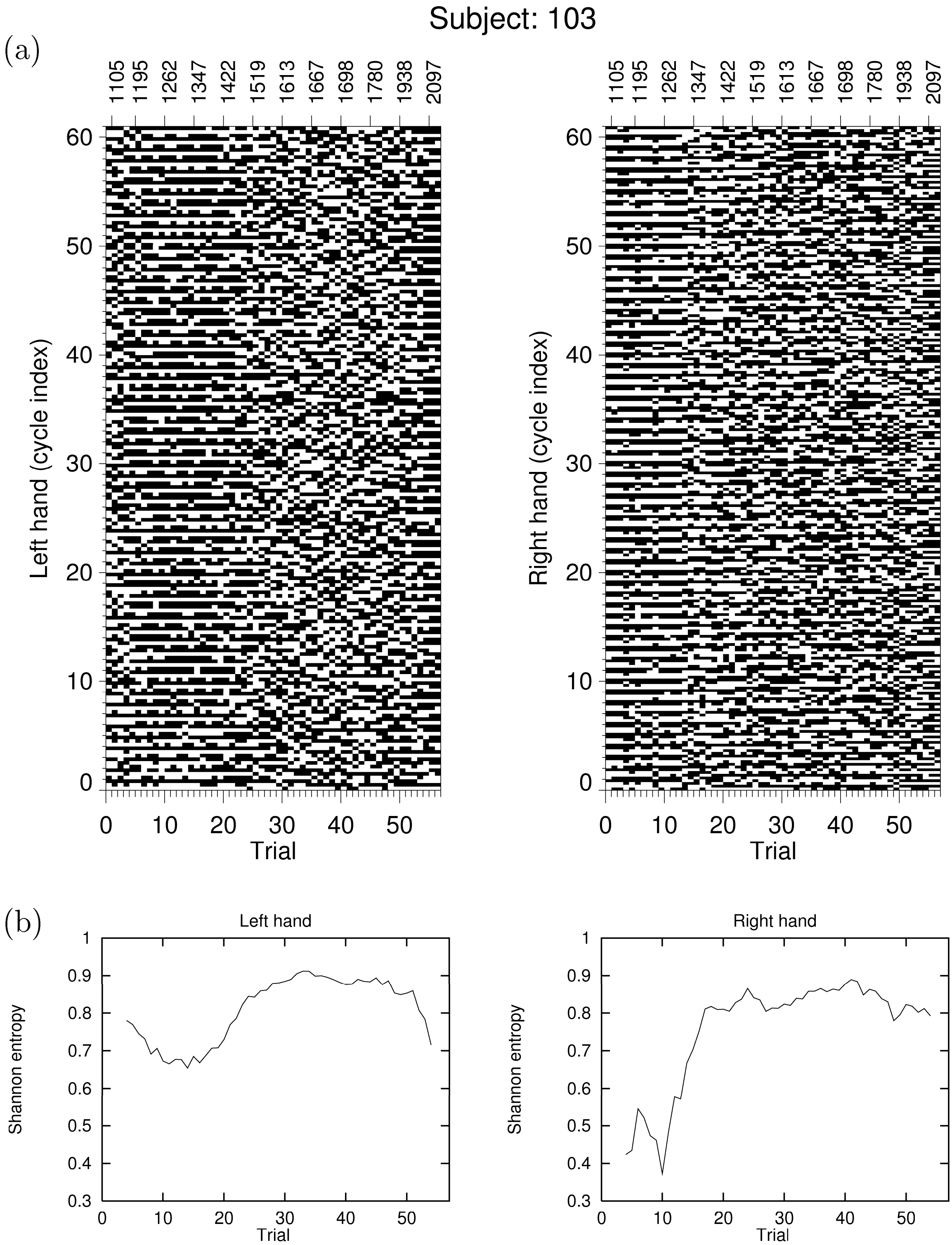

Figure 5: See caption of Fig. 3

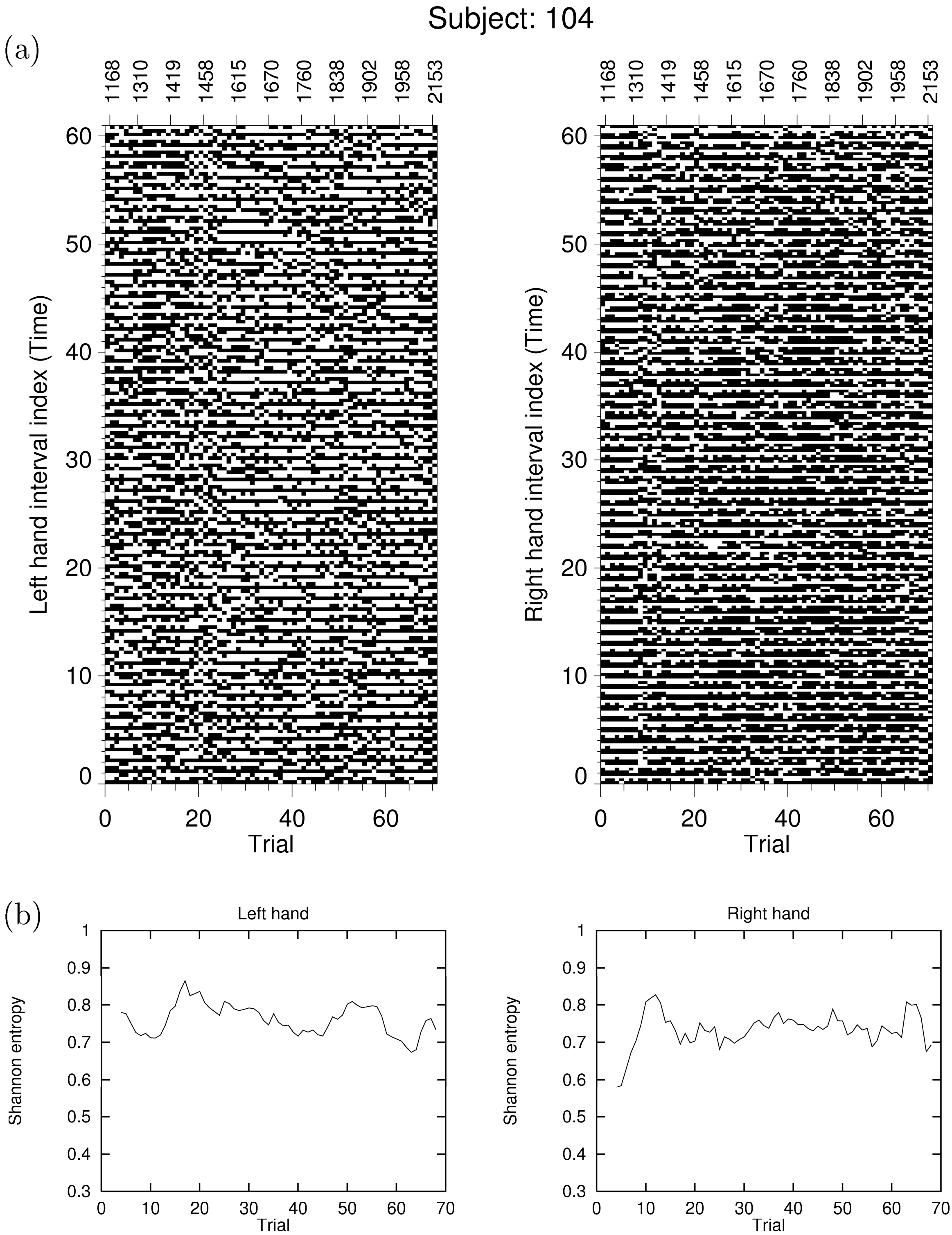

Figure 6: See caption of Fig. 3

Similarly to the 2–symbol representation of the visually delayed tracking data, the correspondence between accuracy of the performance and disorder in the symbol pattern, can be proved using a refinement in the coding rule. In fact, like a good performance, also a time series with irregular but large oscillations around the required values, i.e. a very poor performance, would produce an irregular pattern. This ambiguity can be solved with the help of a 3–symbols coding.

4.3 3–symbols coding

In order to visualize the accuracy of the performances of the task, a third symbol is introduced in the symbol transformation of the relative deviations of Eqs. (13): '2' is assigned to relative deviations whose absolute value is smaller than 5%:

$$s'_n = \begin{cases} 0, & \text{if} \quad r_i^k \text{ or } l_j^k \quad < -0.05 \\ 1, & \text{if} \quad r_i^k \text{ or } l_j^k \quad > 0.05 \\ 2, & \text{if} \quad |r_i^k| \text{ or } |l_j^k| \quad \leq 0.05 \end{cases} , \tag{14}$$

where again $n = 4(k-1)+i = 1, 2, 3, ..., 244$ for the right hand or $n = 3(k-1)+j = 1, 2, 3, ..., 183$ for the left hand. '2' in the 3–symbols patterns corresponds to grey. As before, to '0' and '1' black and white are assigned, respectively. The three–symbols pattern of subject 101 (the same as in Fig. 3 (a)) is shown in Fig. 7. The correspondence between the disordered regions of the 2–symbols patterns and the frequency of grey symbols in the 3–symbols patterns is evident. Thus, the irregular structure observed for small values of the control parameter corresponds to a more accurate performance of the task. The 3–symbol patterns produced by subject 102 are shown in Fig. 8. The disordered structure revealed for fast tempi in Fig. 4 (a) corresponds to a more accurate performance. The relation between disordered structures in two–symbols patterns and accuracy has previously been demonstrated for the 12–cycles polyrhythmic data [Engbert et al. 1997], too.

5 Measures of complexity

The Shannon entropy has proved to be appropriate for the characterization of phase transitions in polyrhythm [Engbert et al. 1997]. In the next section, the probability distribution of words composing the symbol sequences obtained by means of the Eq. (13) will be assessed. Then, the transitions between different regimes will be quantitatively distinguished using the Shannon entropy [Shannon & Weaver 1949].

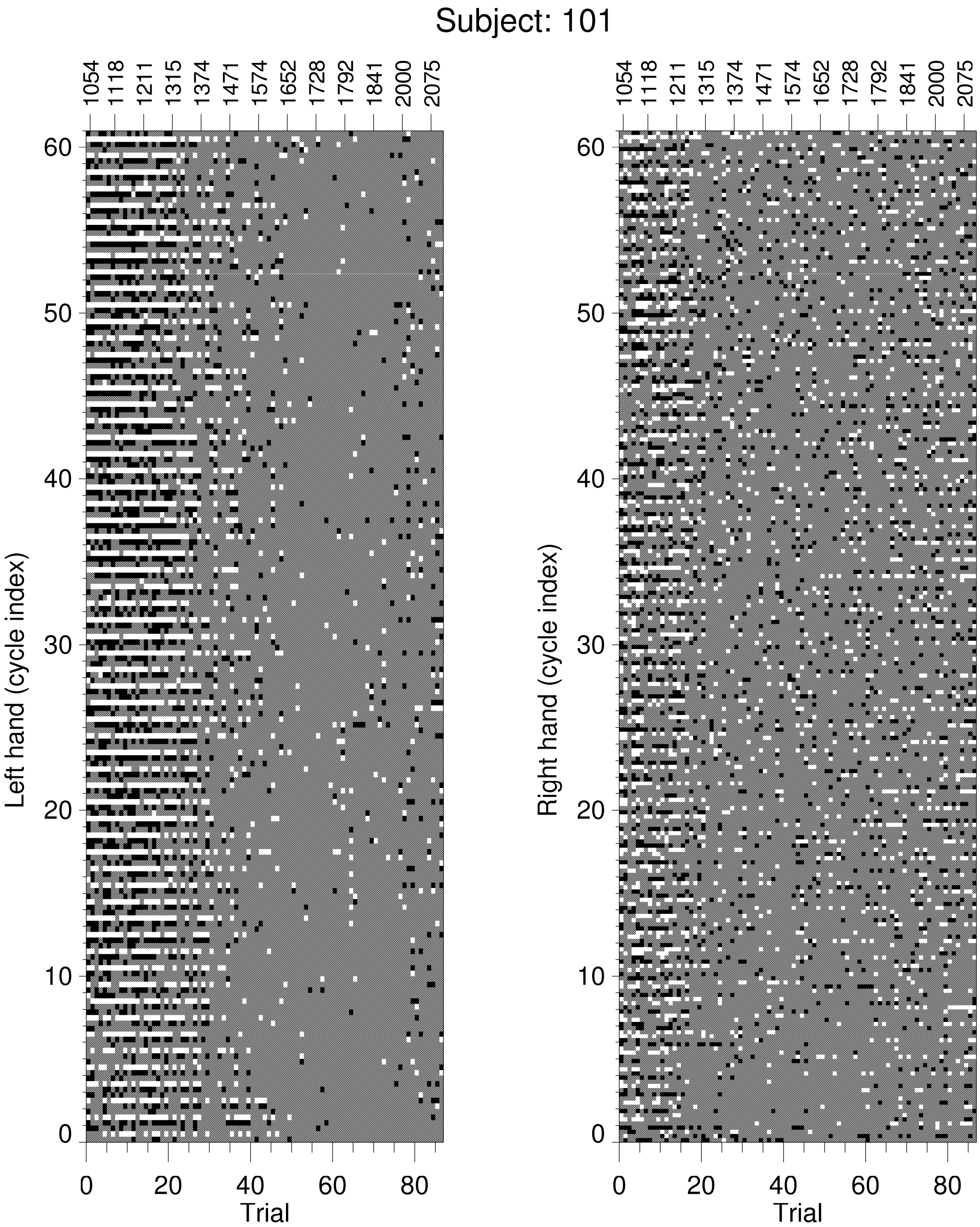

Figure 7: 3–symbol patterns for all the trials of subject 101 obtained by means of the coding rule of Eq. (14). The relation between frequency of grey symbols and irregularity in the 2–symbols pattern of Fig. 3 (a) is evident.

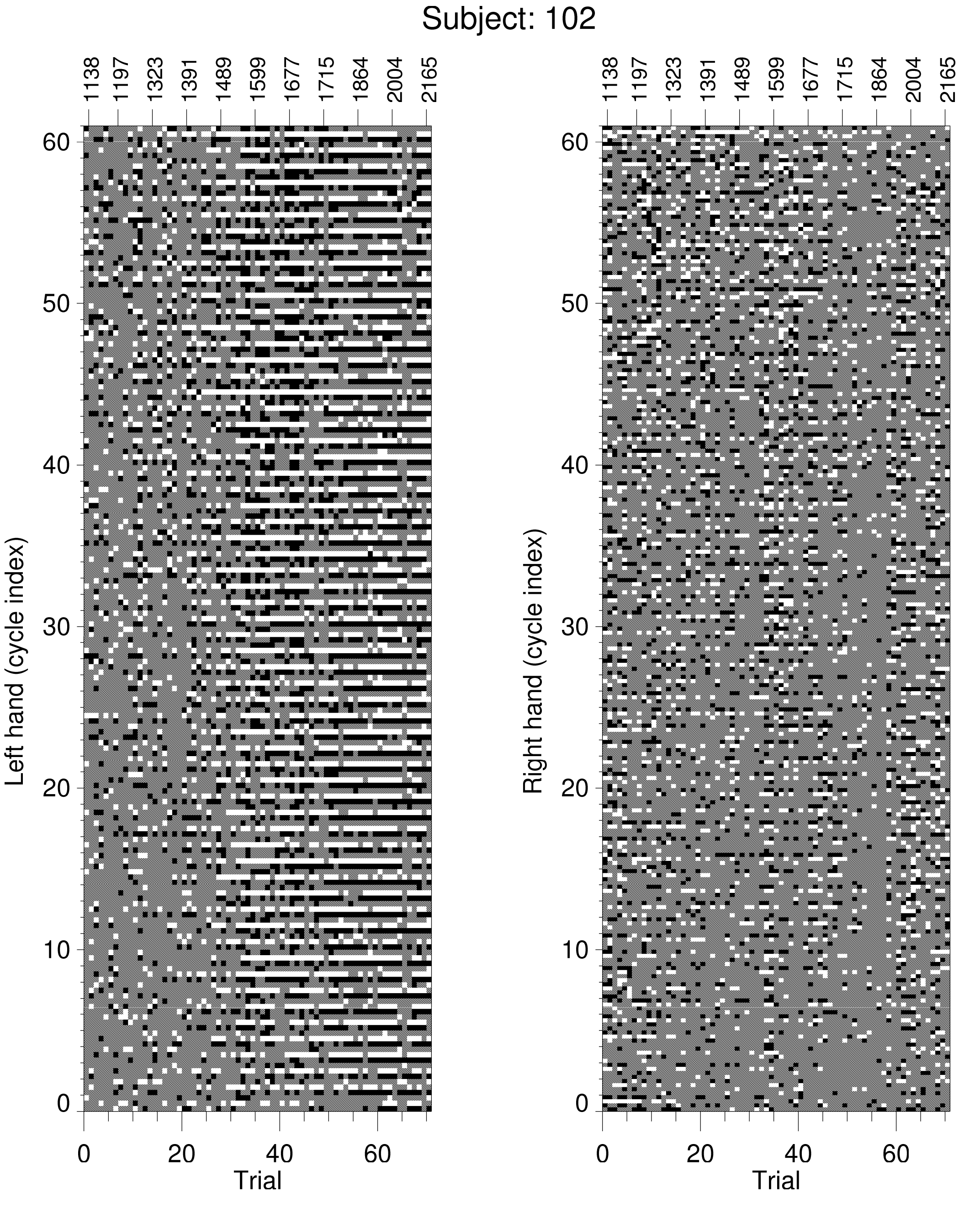

Figure 8: 3–symbols patterns of subject 102. This subject performs the task more accurately at fast tempi ($T < 1490$ ms). This shows that a poor performance cannot be solely due to motoric constraints.

5.1 Word statistics

In order to obtain the probability distribution of words in the symbol patterns, the frequency of all possible words of a certain fixed length are counted. The possible combinations one can get with 2 symbols are $2^4 = 16$ words of length 4 (right hand) and $2^3 = 8$ words of length 3 (left hand). The design of the task leads to a "natural" word length: 4 symbols for the right hand and 3 for the left hand. Due to the transformation of Eqs. (11-12), words composed exclusively of '0' or '1' (all intervals within a cycle are too long or too short) cannot occur, since from the definition of the relative deviations it follows that:

$$\sum_{i=1}^{4} r_i^k = \sum_{j=1}^{3} l_j^k = 0, \qquad k = 1, ..., 61 \ . \tag{15}$$

Consequently, the possible words occurring in the 2–symbol sequences are $N_w^R = 2^4 - 2 = 14$ for the right hand and $N_w^L = 2^3 - 2 = 6$ for the left hand. The frequency p_w of a given word w at a certain realized tempo is computed by counting how many times $N_w^{R,L}$ this word occurs in the sequence and dividing by N (number of words contained in a sequence): $p_w^{R,L} = N_w/N$. Since the length of the words is 4 (right hand) and 3 (left hand) respectively, the number of (non overlapping) words in a sequence is equal to the number of cycles.

The probability distribution of the words is estimated using the relative frequency p_w. About the confidence of such evaluation see [Grassberger 1990]. In general, given a sequence coded using an alphabet of α symbols, α^l is the number of possible words of length l one can find in the sequence. The exponential increasing of this number with l causes a restriction in the choice of l in the case of limited sequences (it should not happen, for example, that $N/l \simeq \alpha^l$, where N is the length of the sequence) [Herzel et al. 1994, Ebeling et al. 1995].

5.2 Shannon entropy

Different probability distributions $p = (p_1, p_2, ...p_{N_w})$ in the symbol sequences are assessed using the Shannon entropy [Shannon & Weaver 1949]:

$$S(p) = -c \sum_{w=1}^{N_w} p_w \ln p_w. \tag{16}$$

$S(p)$ is normalized with respect to the number of possible words by the coefficient $c = 1/\ln N_w$. The Shannon entropy vanishes for a δ–shaped distribution consisting of one word w_0 ($p_w = \delta_{ww_0}$), and has its maximal value (1) for the uniform distribution ($p_w = 1/N_w$).

The Shannon entropy of the word distributions related to the symbol patterns of the four subjects is shown in Figs. 3–6 in (b). The transitions visually revealed in the symbol patterns (Figs. 3–6 in (a)) are well described by the curve of the Shannon entropy: the word distribution characterizing irregular regions corresponds to a large value of the Shannon entropy. Vice versa, small values of the Shannon entropy correspond to regular structures. The Shannon entropy is actually ideal to assess the chance in a distribution. Therefore it suites to the characterization of the transitions from irregular to regular patterns. The transitions of the curve of the Shannon entropy account for transitions in the rhythmic structure due to the variations of the tempo.

Other linear measures for the accuracy of the performance, as for example covariance, do not reveal the transitions as clearly as it can be done using the Shannon entropy [Engbert 1998] . Other measures of complexity like algorithmic complexity [Wackerbauer et al. 1994] have been also applied on these data and have given consistent results.

6 Testing for stationarity

In transforming a time series into a symbolic string, a considerable amount of information is discarded. Nevertheless, if the transformation is shrewdly chosen, the main properties of the underlying dynamics can be captured by the symbol sequence [Hao 1991]. In Sec. 4.2, the R and L intervals have been at first transformed into sequences of relative deviations. Each interval was compared with the instantaneous realized cycle (see Eqs. (11–12). In this way, trends and fluctuations within the trials are not considered. Then, the relative deviations have been transformed into symbol strings, by assigning '0' or '1' to each relative deviation: negative ("too short" interval) or positive ("too long"), respectively. In the symbol patterns obtained using this coarse–graining procedure, phase transitions occur, depending on the external control parameter. These transitions reflect qualitative changes in the behavioral dynamics. Due to the transformation of Eqs. (11–12), the relative deviations reflect the rhythmic structure within the single cycle and do not represent an absolute measure of accuracy of the performance. In other words, the information regarding the dynamics of the overall performance is discarded. Thus, the stationarity of the polyrhythmic data will be investigated in the following.

6.1 Stationarity

The investigation of natural phenomena is accomplished through experiments based on measurements of observable quantities. The weakest concept of *stationarity* requires that the parameters of the system and the parameters of the external set–up are constant during the measurement. In dealing with probabilistic processes, stationarity implies that the probability distributions of the system's variables does not depend on time.

In most of cases, one has not direct access to the system of interest, so that it is difficult to check whether the parameters are constant or not. Thus, an alternative definition of stationarity is used, which is based on the analysis of the available data recording the temporal evolution of the relevant variables of the system.

Let us consider a time series X_t, a sequence of a real variable, where $t \in N$ is the discrete time–index and N denotes the set of integers. The time series X_t is said to be *strictly stationary* if for any n-tuple $t_1, t_2, t_3, ..., t_n$ and for any integer k, the n–dimensional distribution function F, with $n = 1, 2, ...$ satisfies the property:

$$F(z_{t_1}, z_{t_2}, ..., z_{t_n}) = F(z_{t_1+k}, z_{t_2+k}, ..., z_{t_n+k}) \tag{17}$$

A less restrictive definition is that of *weakly stationary* (or *second–order stationary*, or *wide–sense stationary*) which requires that the first two moments exist and are independent on time:

$$< X_t >= \mu \qquad < ((X_t - \mu)^2 >= \sigma^2 \tag{18}$$

where $< \cdot >$ is the ensamble average, and μ and σ are independent on t. Further, the autocorrelation function $\rho(s,t) =< (X_t - \mu)(X_s - \mu) > /\sigma^2$ has to be dependent only on the relative time delay $\tau = t - s$.

Except for some particular cases, it is generally very difficult to investigate the distribution function of a series of observables. Thus, in time series analysis, the concept of stationarity in the weaker sense is mostly used.

The change in the dynamics of the system of interest during the observation period can be checked by measuring some statistical properties in different temporal segments of the signal recording the underlying dynamics of the system itself. If they are different beyond their statistical fluctuations for the different segments, the analyzed time series is not stationary.

Due to the limited length of the polyrhythmic time series here analyzed, stationarity cannot be tested using the standard methods [Isliker & Kurths 1993, Schreiber 1997, Witt et al. 1998]. In the next sections, the stationarity of the data is checked using the Chi–square test [Press et al. 1992]. In particular, the cycle durations $T_1, T_2, ..., T_{61}$ will be tested.

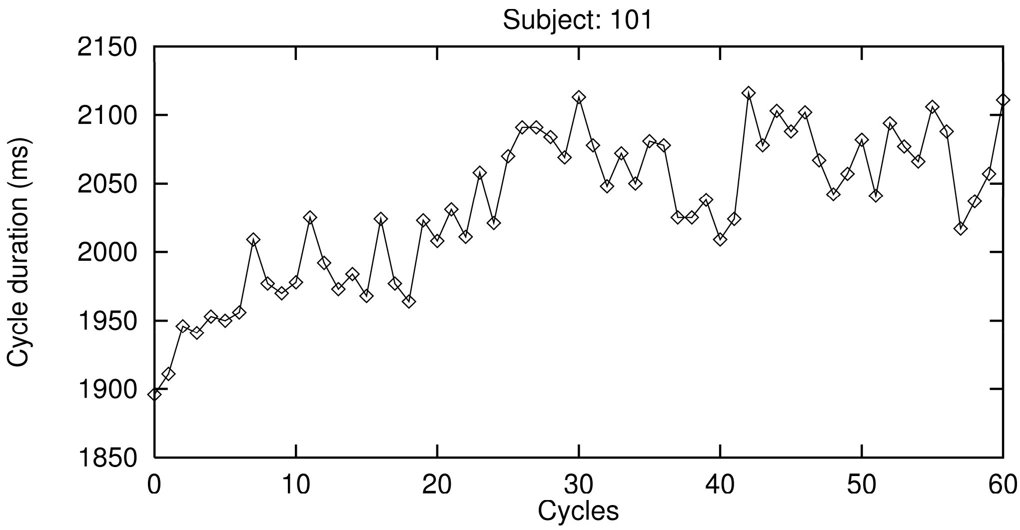

Figure 9: Time series of the cycle durations. The initial given tempo is $T = 1900$ ms, and the cycle duration averaged over the whole trial is $\langle T \rangle = 2033$ ms.

6.2 Time series of cycle durations

The Chi–square test will be applied to the binned distributions of the cycle durations, in different epochs within the trials.

At first, each series of cycle durations $T_1, T_2, ..., T_{61}$ (see Fig. 9) has been reordered by means of a ranking procedure [Press et al. 1992], and than rescaled, in order to gain a normalized time series whose values range from 1/61 to 1. The rescaled cycle durations of all the trials performed by the four subjects are plotted in Fig. 10 with the help of a black and white scale (black = 'min', white = 'max'). The ranking procedure was necessary in order to visualize the time series produced at different tempi in a common scale.

Like the symbol patterns, the trials are graded on the abscissa with respect to the realized tempo. Time is increasing on the ordinate. Arising of dark or light thickening indicates a faster or slower performance with respect to the averaged realized cycle length, respectively.

This visualization of the cycle time series already underlines the overall tendency of the performance within the trials. Nonstationarity is clearly observed in the cycles durations produced by the subjects 101 and 103. The realized tempo becomes slower and slower in trials with fast mean realized tempi. In the patterns of the subjects 102 and 104, no clear tendency can be observed in dependence on the control parameter: the cycle durations become shorter or longer in sequences adjacent in the pattern.

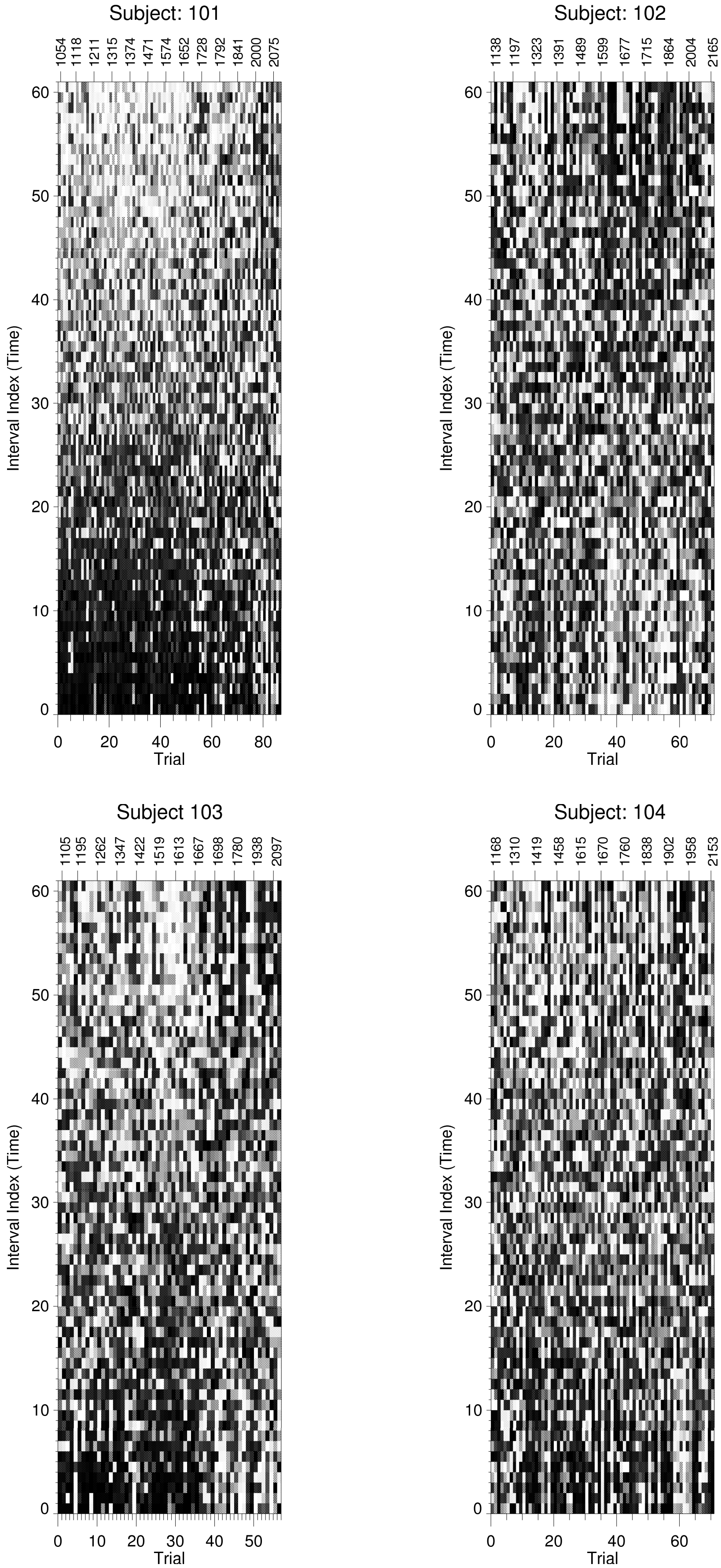

Figure 10: Patterns of the cycle durations represented in a black and white scale. The trials are graded on the abscissa with respect to the mean realized tempo, while the time is increasing on the ordinate. Arising of dark or light thickening indicates a faster or slower performance, respectively, with respect to the average realized cycle duration. The mean realized tempo are indicate on the top in a ms scale.

In the following section, the variations occurring in the distribution of cycle duration along the trial will be investigated. With the help of the well known Chi–square test, the stationarity of the data will be checked.

6.3 Chi–square test

Let us consider two distributions consisting of two binned data sets, and let us suppose one wants to test if the two distributions are different. More precisely, one is interested in checking the assumption that the two distributions are drawn by the same distribution function. D_b^1 and D_b^2 are the numbers of events in the *b–th* bin of the two distributions. The Chi–square statistics is defined as

$$\chi^2 = \sum_{b=1}^{N_B} \frac{(D_b^1 - D_b^2)^2}{D_b^1 + D_b^2}. \tag{19}$$

where N_B is the total number of bins. A large value of χ^2 indicates that the two distributions are different, i.e. that the null hypothesis, affirming that the two sets are drawn by the same probability function, is unlikely. The significance of the Chi–square test is estimated using the *Chi–square probability function* $Q(\chi^2|\nu)$, giving the probability that the sum of the squares of ν random normal variables of unit variance and zero mean is larger than χ^2 [Press et al. 1992].

The interval [0:1] has been divided in 10 bin each 1/10 large. The duration of the whole trial (61 cycles) has been divided in four equal windows each containing 15 cycles (the last was neglected). For each time window, the binned distribution of the cycle durations of all trials has been computed. This way, four distributions have been obtained, corresponding to the four windows shown in the sketch on the left in Figs. 11–14 in (b). The four distributions have been mutually tested in order to check the null hypothesis of being drawn by the same probability function. The results of the test for all subjects are shown in Figs. 11–14 in the first column (b). In the first column (a) the pattern of the tested cycle durations is shown. Two tested distributions are significantly different if their Chi–square is associated with a probability smaller than 10^{-3}. The probability is represented in a 4x4 matrix with the help of three colors: black if the two distributions are not significantly different ($p > 10^{-3}$), grey and white ($10^{-4} < p < 10^{-3}$ and $p < 10^{-4}$, respectively) if they are significantly different. The test has revealed nonstationarity: each distribution is significantly different at least from two other distributions.

A lot of methods of data analysis require stationarity of the time series. Symbolic dynamics is a useful method in dealing with nonstationary data, too. Through the transformation into relative deviations of Eqs. (11–12), due to the coarse–graining procedure, the phase transitions induced by the external control parameter are

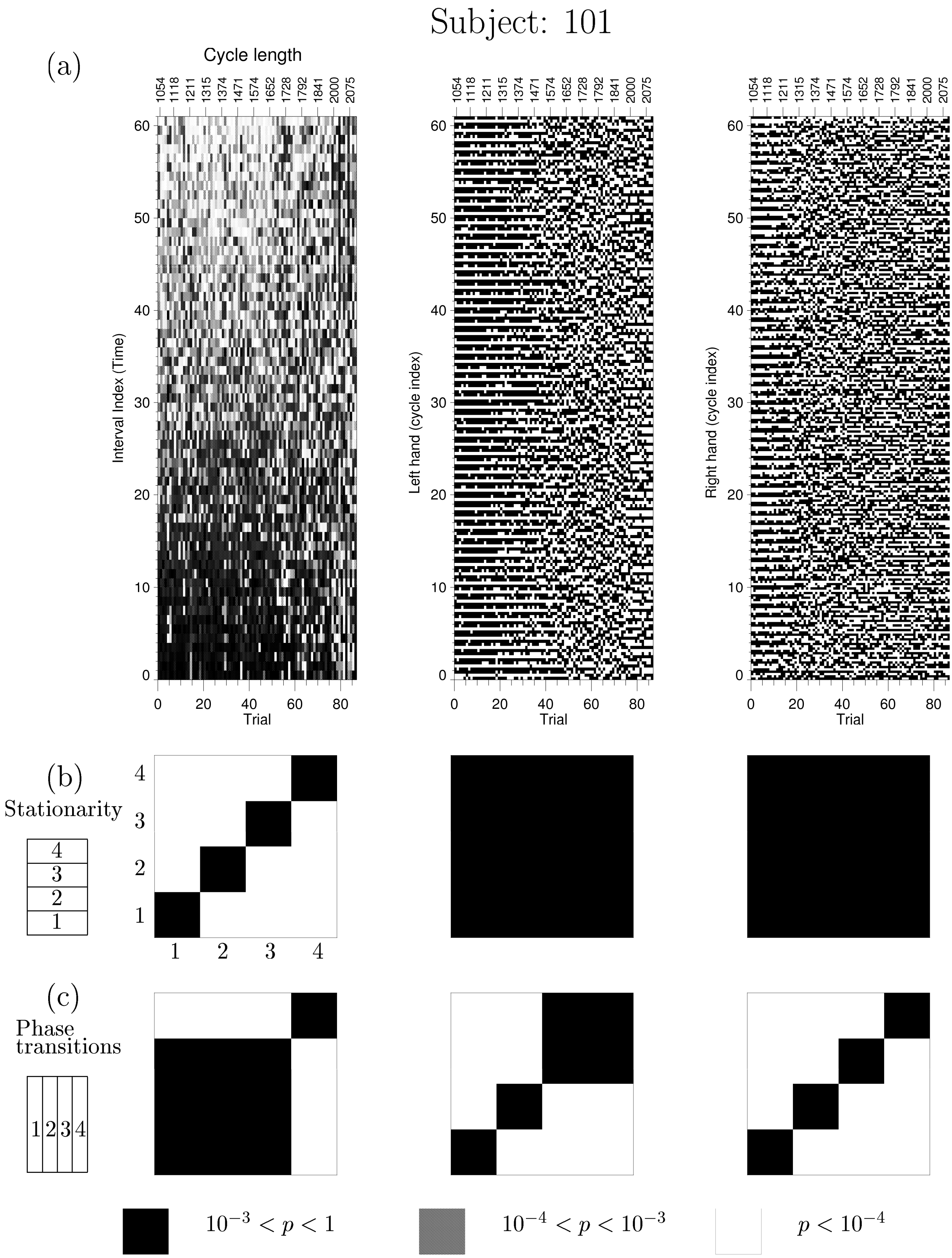

Figure 11: Results of the Chi–square test for the data produced by subject 101.

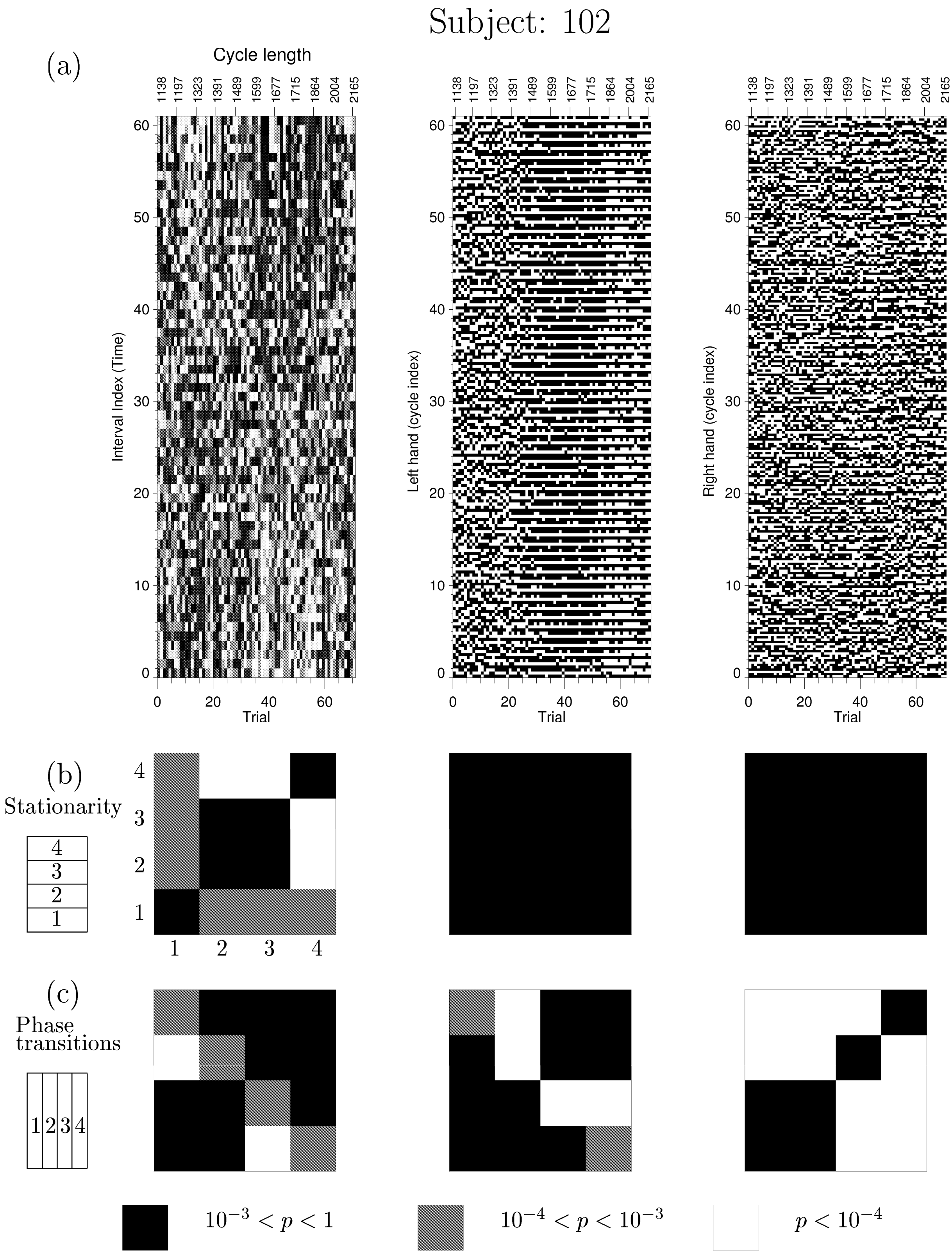

Figure 12: Results of the Chi–square test for the data produced by subject 102.

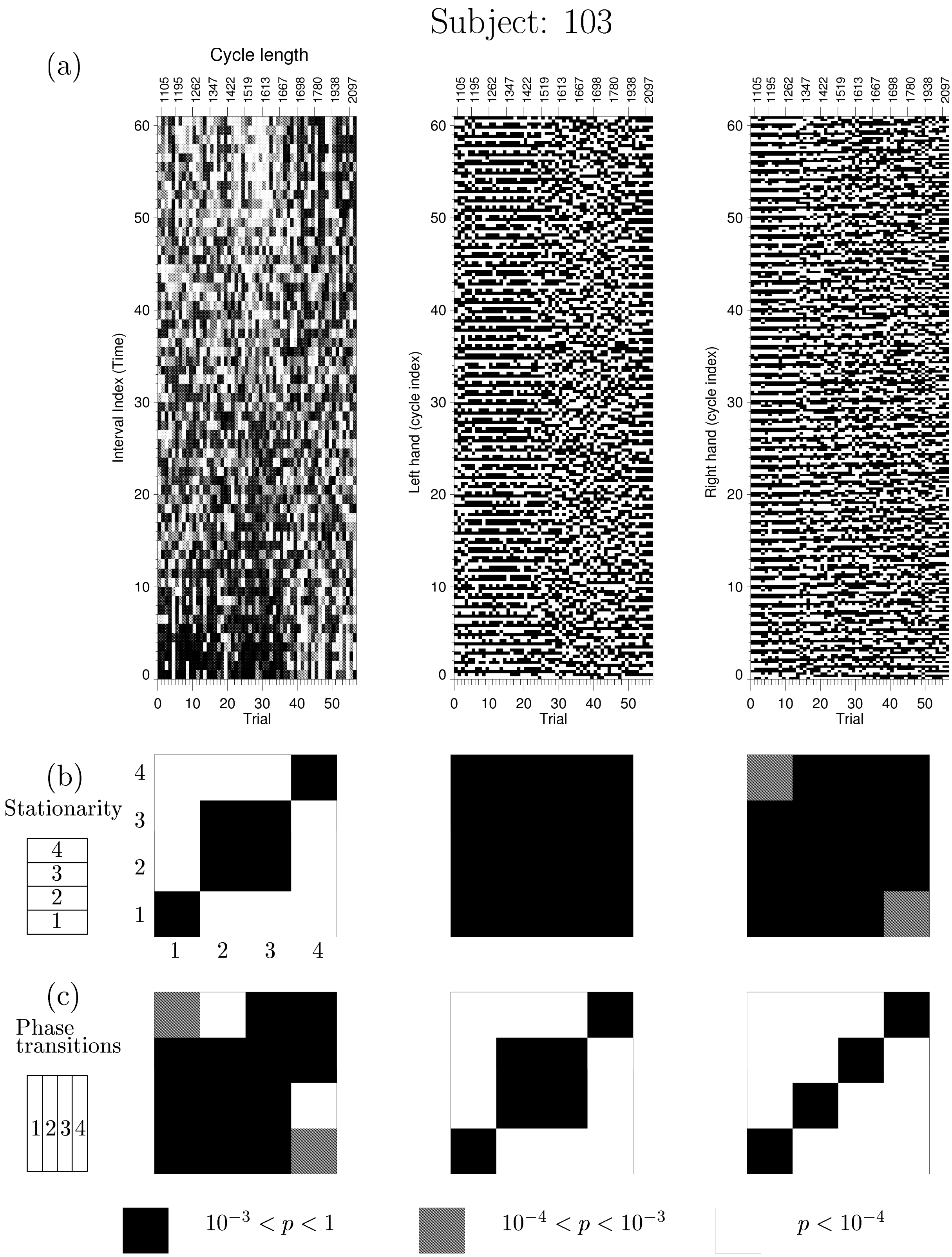

Figure 13: Results of the Chi–square test for the data produced by subject 103.

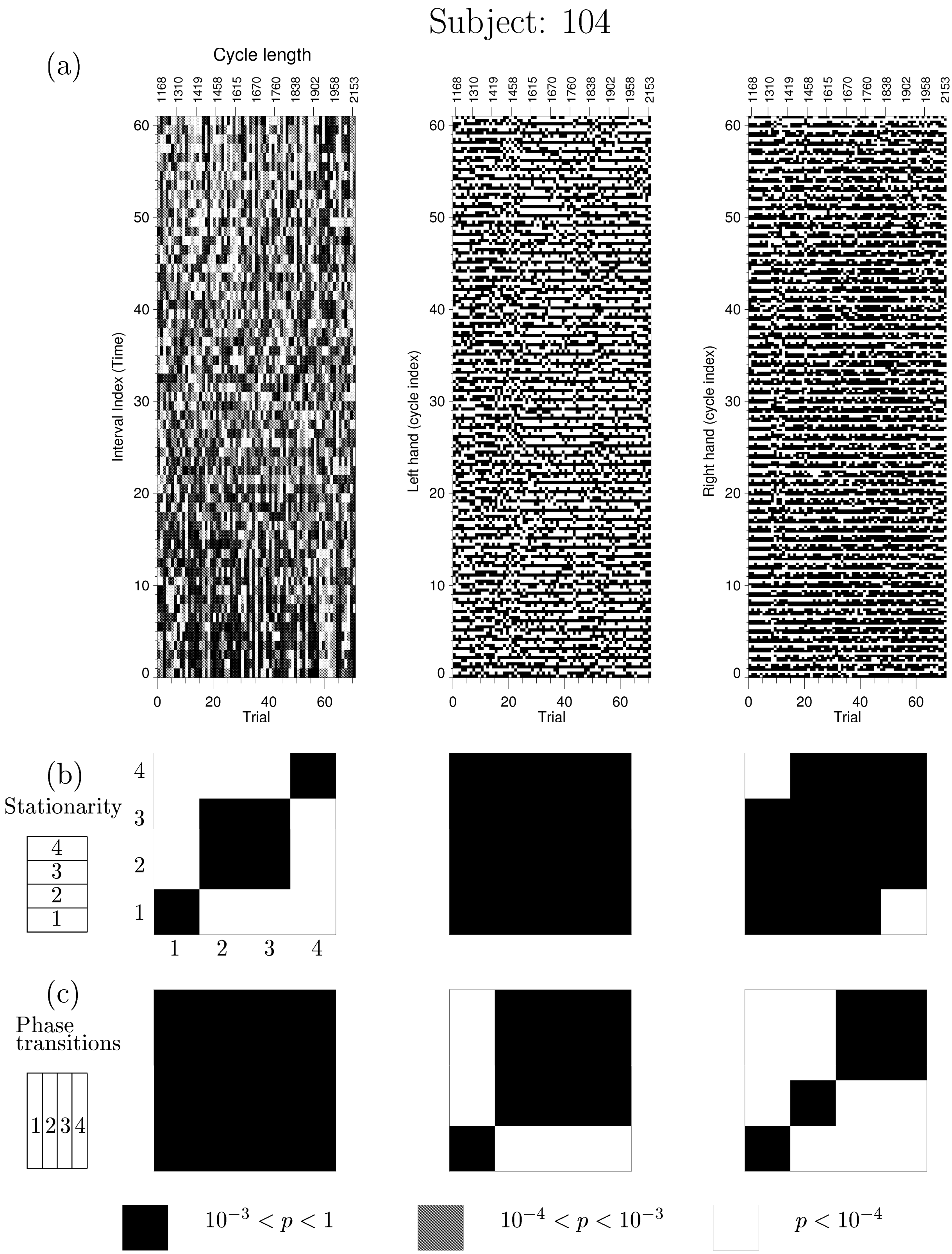

Figure 14: Results of the Chi–square test for the data produced by subject 104.

clearly visualized in the symbols patterns. The Chi–square test has been performed also on the 2–symbols patterns of the R and L intervals. In this case, the distributions of the words of length 4 (for the right hand) and 3 (left hand) (see Sec. 5.1) have been tested. The matrices representing the probability obtained for the same windows used for the distributions of the time durations are shown in Figs. 11–14 in (b) in the second and third columns. As expected, the null hypothesis is almost overall rejected. In particular, the distributions are not significantly different in all cases for the left hand (second column) and in almost all cases for the right hand (third column). The former, in fact, shows generally a more robust rhythmic structure.

Finally, the variations of the distributions along the abscissa has been tested. All tempi have been divided in four equal subsets (the remainders have been neglected), and for each subset the distribution of the cycle durations of the whole trial has been computed [2] (see Figs. 11–14 (c) sketch on the bottom left). The results show that significantly different distributions of cycle durations and 2–symbols words emerge along the abscissa. As expected, the significant transitions observed in the symbol patterns (second and third column (c)) do not necessarily correspond to significant transitions of the distribution of the cycle duration. (first column (c)).

7 Control parameters in the production of rhythms

The observation of phase transitions in the symbol patterns (Sec. 4) and the detection of the nonstationarity of the cycle durations (Sec. 6) are interesting results for the dynamical model proposed by Engbert et al. [1997]. The model describes the production of polyrhythms of arbitrary order N^L:N^R. Nonlinear error is the basic mechanism for explaining the phase transitions of the system. The duration of the k–th cycle is given by a stochastic variable (timekeeper). This value is dynamically modified by an error correction term, which operates on the deviation of the previous interval from the target interval. A coupling term maintains the synchronization of the hand movements. The intervals R and L, produced in the k–th cycle, are generated by coupled maps. The control parameters of the system are functions of the tempo of performance (the strength of the correction mechanism and of the coupling). Varying the control parameters, a period–doubling bifurcation occurs, which generates the periodicity of the symbol patterns observed in the data.

The difficulty in choosing the reliable control parameters in experimental psychology has already been pointed out in Sec. 4. Unlike in many physical experiments, external parameters are more difficult to control in psychological systems. In the case of rhythms production, the identification of the control parameter inducing the

[2] Due to the ranking procedure, the distribution of the cycle durations calculated over the whole trials is a uniform distribution. Therefore, for testing the stationarity of the cycle durations, the first half of the time series has been investigated (cycles 1 to 30).

phase transitions is not obvious: is it the tempo the subject is required to perform, i.e. the tempo initially given by the computer, or the tempo the subject really produces? In Sec. 4 the symbol patterns of the R and L intervals have shown that the deviation from the prescribed rhythmic structure is remarkably stable after the first cycles, although, as the test for stationarity has proved, the cycle duration fluctuates. This finding argues for the dissociation between "intentional" and stochastic variations of the realized tempo. In other words, the tempo initially realized determines the rhythmic pattern which is not affected by successive fluctuations of the cycle duration.

8 Analysis of relative phases

In the case of the polyrhythmic time series, the derivation of the relative phases is an alternative way to investigate the behavior of the system by varying the control parameter. Through the relative phases, the dynamics of the coordination of the hands is taken into account: one locally focuses on the mutual relation between strokes performed by the hands within a cycle.

The relative phases are computed by taking the right hand as a reference. The phase of the left hand is supposed to increase linearly from 0 to 2π in the interval between two strokes. The phases of the left hand with respect to the first, second and third strokes performed by the right hand are obtained directly from Fig. 15: phase I $= 3/2\pi$, phase II $= \pi$ and phase III $= 1/2\pi$ (first, second and third stroke of the right hand, respectively).

In Fig. 16 the relative phases for all the trials produced by subject 102 are plotted with the help of a continuous color scale. The latter ranges in an interval centered on the prescribed value of 0.75 (phase I), 0.5 (phase II) and 0.25 (phase III), respectively. The scale is expressed in 2π, e.g. 1 means 2π, 0.75 means 3/4 of 2π and so on. The prescribed value of the relative phase corresponds to light blue. Green corresponds to "left hand late" and dark blue to "left hand in advance" with respect to the right hand. The 2–symbol patterns for the subject 102, plotted in Fig. 4 (a), has shown the arising of periodic sequences (i.e. inaccurate performance) for slow tempi (after the first 20 cycles). In the pattern of phase I, one observes that in this region the left hand is in advance with respect to the right hand. This corresponds to the thickening of green on the right side of the pattern shown in (a). Phase II (in (b)) oscillates around the expected value. A slight transition similar to the one occurring in phase I is visible for slow tempi ($\langle T \rangle > 1800$ ms. Phase III (in (c)) shows an opposite tendency with respect to the pattern of phase I: the left hand is too late with respect to the second stroke of the right hand.

The patterns of the relative phases of subject 104, shown in Fig. 17, shows a peculiar systematic error in the phase III (shown in (c)). Although no clear order–disorder

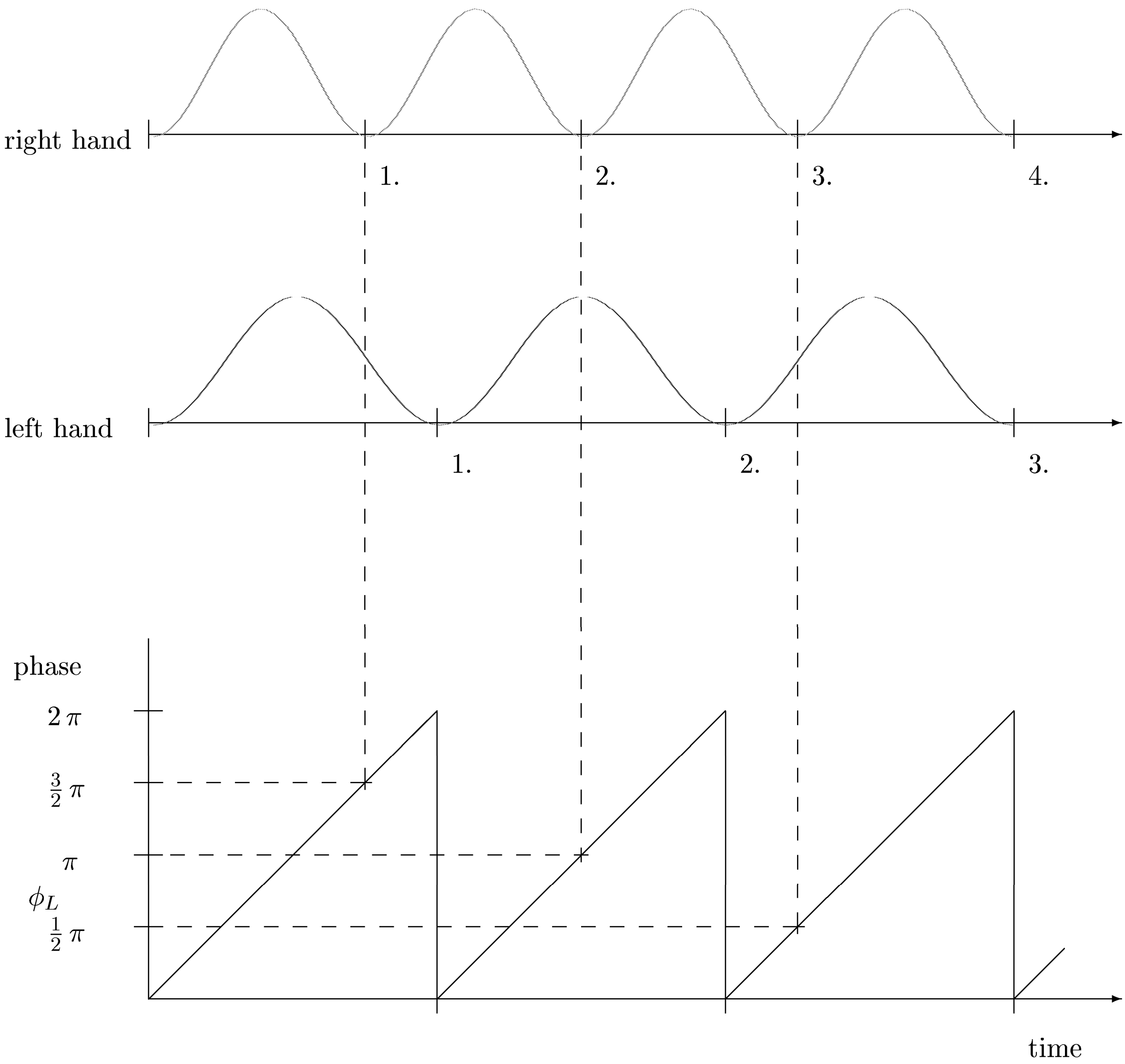

Figure 15: Computation of the three relative phases of the left hand with respect to the right hand. It is assumed that the phase of the left hand increases monotonously from 0 to 2π between two successive strokes (after: Engbert et al. [1997]).

(a)

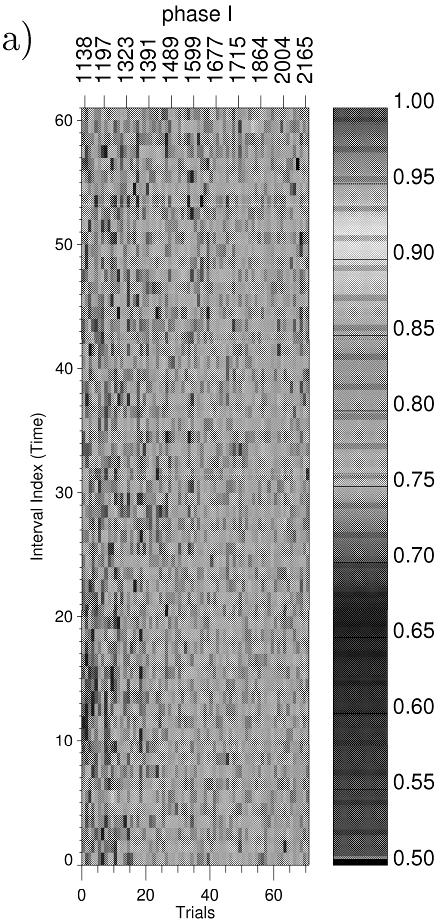

(b)

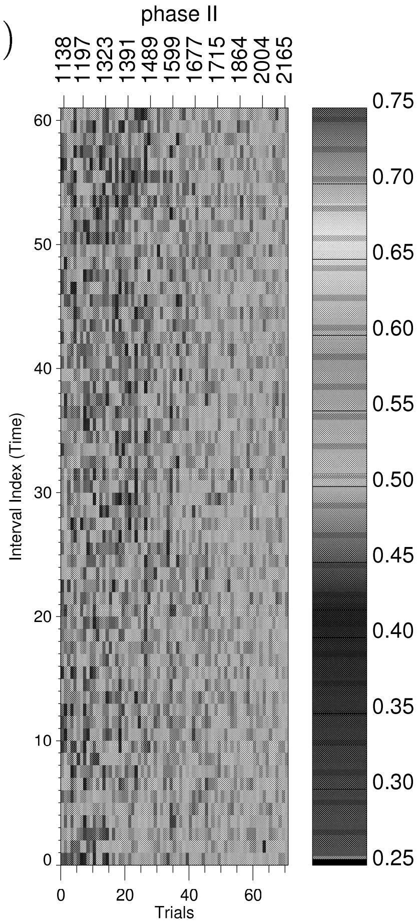

(c)

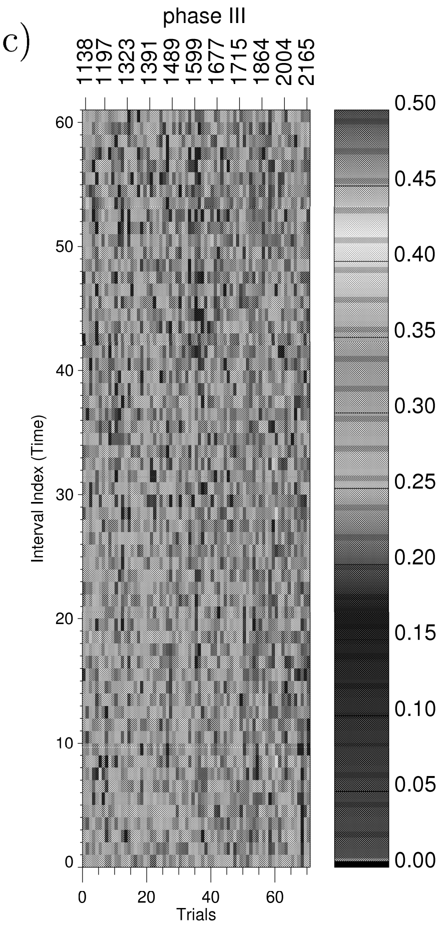

Figure 16: Patterns of the relative phases of subject 102. The color scales are centered on the expected values (0.75, 0.5 and 0.25, respectively), which corresponds to light blue. The scale is in 2π unity. Green and dark blue correspond to inaccurate performances.

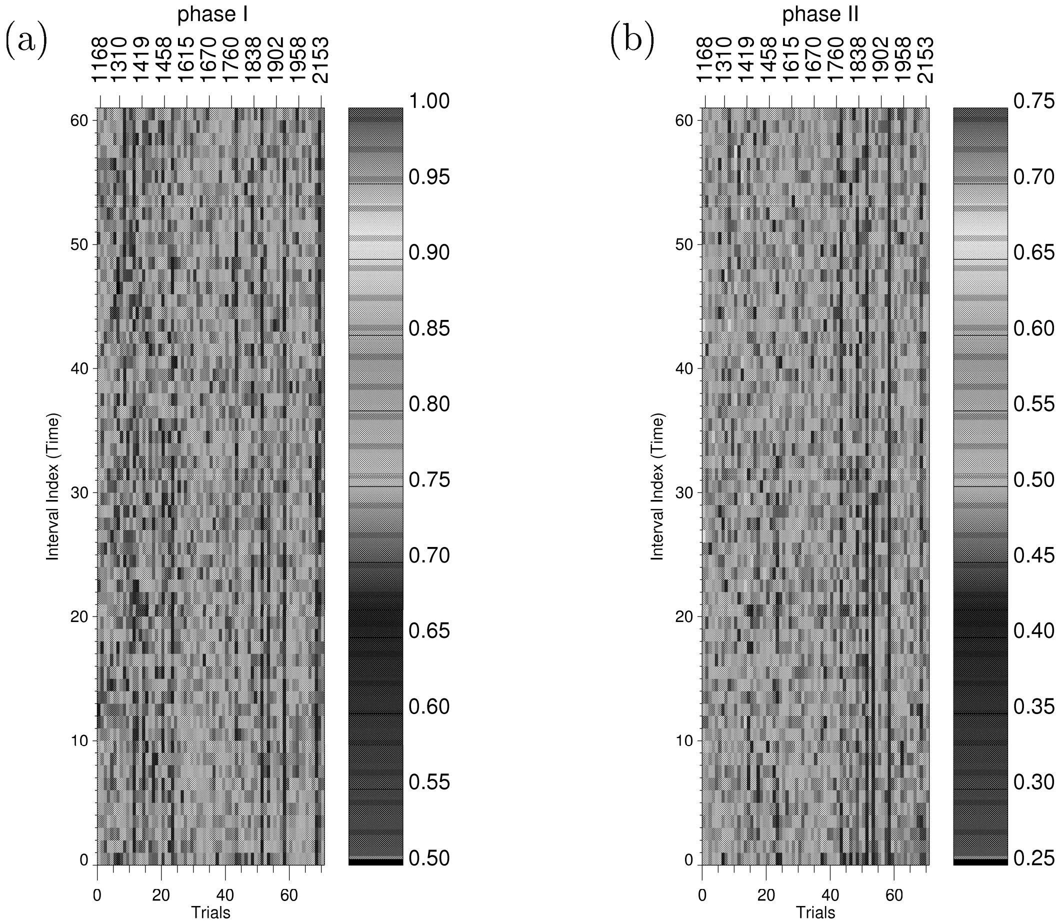

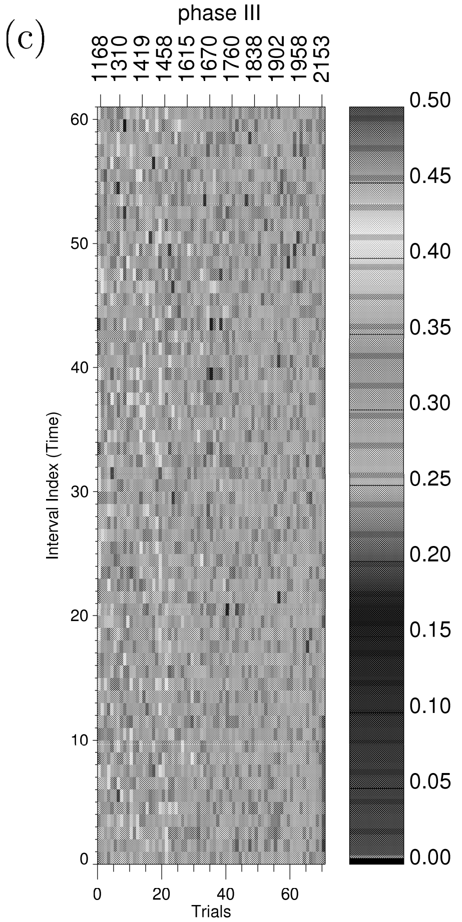

Figure 17: Relative phases of subject 104 (see caption of Fig. 16).

transition occurs in the 2–symbol patterns of the R and L intervals produced by this subject (illustrated in Fig. 6 (a)), the relative phase III does show, in this representation, a quite sharp transition dividing the pattern in two regions: for slow tempi ($\langle T\rangle > 1500$ ms) it oscillates around the prescribed value. For $\langle T\rangle < 1500$ ms the left hand turns to be systematic in advance with respect to the right hand.

The patterns of the relative phases allow the visualization of the dynamics of the coordination of the hands. This aspect is softed in the symbol patterns of the R and L intervals. Preliminary attempts of applying symbolic transformation to the relative phases did not provide further insights. Future efforts should aim to investigate the relative phases using other methods of analysis.

9 Discussion

The application of symbolic dynamics to the polyrhythmic data has provided important results. Despite the intrinsic fluctuations of the data, using the coarse-graining transformation applied in Sec. 4, robust properties of the underlying dynamics have been extracted. In the symbol patterns of the relative deviations, transitions induced by the externally varied tempo are revealed. Order–disorder transitions in the symbol patterns reflect transitions in the quality of the performance: from an incorrect to a correct timing of the polyrhythm. The observed transitions are quantitatively described using the Shannon entropy (Sec. 5).

The qualitative transitions in the production of polyrhythms argue against the linear statistical models proposed for the description of simple movement tasks [Vorberg & Wing 1996]: since linear models cannot account for the qualitative changes observed in the data, a nonlinear mathematical description is necessary [Engbert et al. 1997].

The stationarity of the data has been tested with the help of the Chi–square test (Sec. 6). Nonstationarity has been revealed in the cycle durations. The stability of the rhythmic structure in trials with fluctuating cycle durations proves that the control parameter has to be identified in the initial tempo carried out "intentionally" by the subjects. The latter is the parameter which is externally manipulated. Its variation is dissociated from the stochastic drift of the cycle duration and solely induces the observed transitions of the symbol patterns.

The analysis of the relative phases of Sec. 8 has focused on characteristics of the strategy of the performance related to the coordination between hands, which are not emphasized by the analysis of the relative deviations.

10 Outlook

The Chi–square test has revealed nonstationarity in the data. In a next step, nonlinearity should be also tested [Theiler et al. 1992, Schreiber & Schmitz 1997, Voss & Kurths 1998]. A polyrhythmic task where the tempo is varied within a single trial will be investigated. The tempo will be systematically increased by the subject and then decreased. This way, one could check whether the rhythmic structure undergoes tempo–induced transitions within a single trial. The occurrence of hysteresis phenomena could also be checked. The success of the analysis of polyrhythms presented here makes symbolic dynamics a promising tool to be applied also to other motor control experiments. The derivation of the relative phases obtained in Sec. 8 has stressed the importance of the aspect of coordination in the task: thus the relative phases should be deeply analyzed.

References

[Badii & Politi 1997] R. Badii & A. Politi, *Complexity: Hierarchical structure and Complexity in Physics.* (Cambridge University Press, 1997).

[Beck & Schlögl 1993] C. Beck & F. Schlögl, *Thermodynamics of chaotic systems.* (Cambridge University Press, 1993).

[Box & Jenkins 1976] G.E.P. Box & G.M. Jenkins, *Time Series Analysis, Forecasting and Control.* (Holden–Day, San Francisco, 1976).

[Deutsch 1983] D. Deutsch, The generation of two isochronous sequences in parallel. *Percept. & Psychophys.* **34** (1983) 331-337.

[Ebeling et al. 1995] W. Ebeling, T. Pöschel & K.-F. Albrecht, Transinformation and Word Distribution of Information-Carrying Sequences. *Int. J. Bif. Chaos* **5** (1995) 51.

[Engbert et al. 1997] R. Engbert, C. Scheffczyk, R.T. Krampe, M. Rosenblum, J. Kurths & R. Kliegl, Tempo–induced transitions in polyrhythmic hand movements. *Phys. Rev. E* **56** (1997) 5823–5833.

[Engbert 1998] R. Engbert, *Nichtlineare Dynamik kognitiv–motorischer Prozesse.* (Dissertation, Universität Potsdam, 1998).

[Grassberger 1990] P. Grassberger, Finite Sample Corrections to Entropy. *Phys. Lett. A* **128** (1990) 369.

[Haken et al. 1996] H. Haken, C.E. Peper, P.J. Beek & A. Daffertshofer, A model for phase transitions in human hand movements during multifrequency tapping. *Physica D* **90** (1996) 179-196.

[Hao 1989] B.-L. Hao, *Elementary Symbolic Dynamics and Chaos in Dissipative Systems.* (World Scientific Publ., Singapore, 1989).

[Hao 1991] B.-L. Hao, Symbolic dynamics and characterization of complexity. *Physica D* **51** (1991) 161-176.

[Hempelmann & Kurths 1990] A. Hempelmann & J. Kurths, Dynamics of the Outburst Series of SS Cygni. *Astronomy and Astrophysics* **232** (1990) 356-366.

[Herzel et al. 1994] H. Herzel, A.O. Schmitt & W. Ebeling, Finite Sample Effects in Sequence Analysis. *Chaos, Solitons & Fractals* **4** (1994) 97.

[Isliker & Kurths 1993] H. Isliker & J. Kurths, A test for stationarity. *Int. J. Bif. & Chaos* **3** (1993) 1573-1579.

[Jagacinski et al. 1988] R.J. Jagacinski, E. Marshburn, S.T. Klapp & M.R. Jones, Tests of parallel versus integrated structure in polyrhythmic tapping. *J. Motor Behavior* **20** (1988) 416-442.

[Kantz et al. 1998] H. Kantz, J. Kurths & G. Mayer-Kress (eds.), *Nonlinear analysis of physiological data.* (Springer, Berlin – Heidelberg – New York, 1998).

[Krampe et al. 1999] R. Krampe, R. Kliegl, U. Mayr, R. Engbert & D. Vorberg, The Fast and the Slow of Skilled Bimanual Rhythm Production: Parallel vs. Integrated Timing. *J. Exp. Psych.: Human Percept. Perform.* in press.

[Kurths et al. 1995] J. Kurths, A. Voss, P. Saparin, A. Witt, H.J. Kleiner & N. Wessel, Quantitative analysis of heart rate variability. *CHAOS* **5** (1995) 88-94.

[Packard et al. 1980] N.H. Packard, J.P. Crutchfield, J.D. Farmer & R.S. Shaw, Geometry from a time series. *Phys. Rev. Lett.* **45** (1980) 712-716.

[Panter 1965] P. Panter, *Modulation, noise and spectral analysis.* (McGraw–Hill, New York, 1965).

[Peper et al. 1995] C.E. Peper, P.J. Beek & P.C.W. van Wieringen, Frequency–induced transitions in bimanual tapping. *Biol. Cybern.* **73** (1995) 301-309.

[Press et al. 1992] W.H. Press, S.A. Teukolsky, W.T. Vetterling & B.P. Flannery, *Numerical Recipes in C.* (Cambridge University Press, 1992).

[Sauer et al. 1991] T. Sauer, J.A. Yorke & M. Casdagli, Embedology. *J. Stat. Phys.* **65** (1991) 579-616.

[Schiek et al. 1997] M. Schiek, F.R. Drepper, R. Engbert, H.-H. Abel & K. Suder, Cardiorespiratory Synchronization. In: [Kantz et al. 1998].

[Schreiber & Kantz 1995] T. Schreiber & H. Kantz, Noise in chaotic data: Diagnosis and treatment. In *CHAOS* **5** (1995) 1-209. (Focus issue: *Dynamical disease: Mathematical analysis of human illness*).

[Schreiber 1997] T. Schreiber, Detecting and Analyzing Nonstationarity in a Time Series Using Nonlinear Cross Predictions. *Phys. Rev. Lett.* **78** (1997) 843-846.

[Schreiber & Schmitz 1997] T. Schreiber & A. Schmitz, Improved Surrogate Data for Nonlinearity Tests. *Phys. Rev. Lett.* **77** (1997) 635-638.

[Schwarz et al. 1993] U. Schwarz, A.O. Benz, J. Kurths & A. Witt, Analysis of Solar Spike Events by Means of Symbolic Dynamics Methods. *Astron. Astrophys.* **277** (1993) 215-224.

[Shannon & Weaver 1949] C.E. Shannon & W. Weaver, *The Mathematical Theory of Communication.* (University of Illinois Press, Urbana, 1949).

[Stevens 1886] L.T. Stevens, On the time sense. *Mind* **11** (1886) 393-404.

[Summers et al. 1993] J.J. Summers, D.A. Rosenbaum, B.D. Burns & S.K. Ford, Production of polyrhythms. *J. Exp. Psychol.: Hum. Percept. Perform.* **19** (1993) 416-428.

[Takens 1981] F. Takens, Detecting strange attractors in turbulence. *Springer Lecture Notes in Mathematics* **898** (1981) 366-381.

[Theiler et al. 1992] J. Theiler, S. Eubank, A. Longtin, B. Galdrikian & J.D. Farmer, Testing for nonlinearity in time series: the method of surrogate data. *Physica D* **58** (1992) 77-94.

[van Kampen 1981] N.G. van Kampen, *Stochastic processes in physics and chemistry.* (North–Holland, Amsterdam, 1981).

[Vorberg & Wing 1996] D. Vorberg & A.M. Wing, Modeling Variability and Dependence in Timing. In: H. Heuer & S.W. Keele (eds.), *Handbook of Perception and Action, Vol. 2.* (Academic Press, London, 1996).

[Voss & Kurths 1998] H. Voss & J. Kurths, Test for nonlinear dynamical behavior in symbol sequences. *Phys. Rev. E* **58** (1998) 1155-1158.

[Wackerbauer et al. 1994] R. Wackerbauer, A. Witt, H. Atmanspacher, J. Kurths & H. Scheingraber, A Comparative Classification of Complexity Measures. *Chaos, Solitons & Fractals* **4** (1994) 133–173.

[Witt et al. 1994] A. Witt, J. Kurths, F. Krause & K. Fischer, On the validity of a model for the reversals of the Earth's magnetic field. *Geophys. Astrophys. Fluid Dynam.* **77** (1994) 79-91.

[Witt et al. 1998] A. Witt, J. Kurths & A. Pikovsky, Testing stationarity in time series. *Phys. Rev. E* **58** (1998) 1800-1810.